PERIODICA POLYTECHNICA SER. MECH. ENG. VOL. 48, NO. 1, PP. 99–110 (2004)

FREE VIBRATION OF THIN-WALLED BEAMS

Gábor M. VÖRÖS

Department of Applied Mechanics
Budapest University of Technology and Economics
H–1521 Budapest, Hungary
e-mail: voros@mm.bme.hu

Received: January 30, 2004

Abstract

Consistent and simple lumped mass matrices are formulated for the dynamic analysis of beams with arbitrary cross-section. The development is based on a general beam theory which includes the effect of flexural-torsion coupling, the constrained torsion warping and the shear centre location. Numerical tests are presented to demonstrate the importance of torsion warping constraints and the acceptable accuracy of the lumped mass matrix formulation.

Keywords: torsion, thin walled beam, mass matrix, free vibration.

1. Introduction

During the torsion of bars an out of section plane, axial warping displacement takes place which is assumed to depend on the change of the angle of twist. The torsional warping has no effect on stresses if the measure of warping is the same in each section including the ends. This implies that the torsional rotation is a linear function along the beam axis. If the torsional rotation is far from the linear distribution, as it is in torsional vibration modes, or the beam ends are constrained, the torsional warping may have an important effect on the static or dynamic response of the beam structure. In addition to the torsion warping effect, the coupling between the bending and the tosional free vibration modes occurs when the centroid (mass centre) and the shear centre (centre of twist) of the beam section are non-coincident.

The thin-walled beam theory was established by VLASOV [1] and TIMOSHENKO and GERE [2]. Among others coupled bending-torsional vibrations of beams have been investigated in recent years by FRIBERG [3] and BANERJE [4]. TRAHAIR and PI [5] summarized a series of investigations on this field. A consistent finite element formulation for the free vibration was presented by KIM [6]. In this paper an exactly integrated consistent and a lumped mass matrices are presented for the 7 DOF finite element beam model. The formulation includes the flexure-torsion coupling and the constrained warping effects.

The equation for free vibration of an elastic system undergoing small deformations and displacements can be expressed in the form

$$\mathbf{K}\,\mathbf{U} + \mathbf{M}\,\ddot{\mathbf{U}} = \mathbf{0},$$

where **K** and **M** are the assembled elastic stiffness and mass matrices respectively, and $\mathbf{U}(t)$ is the set of nodal displacements. The dot represents the time derivative.

2. Kinematics of Beam

Fig. 1 shows the basic systems and notations. The local x axis of the right hand orthogonal system is parallel to the beam straight axis and passes trough the $\mathbf{N}_1$ $\mathbf{N}_2$ element nodes of the finite element mesh. The axes y and z are parallel to the principal axes, signed as r and s. The position of the centroid **C** and shear centre **T** relative to the node **N** in the plane of the section is given by the co-ordinates y_{NC}, y_{CT} and z_{NC}, z_{CT}.

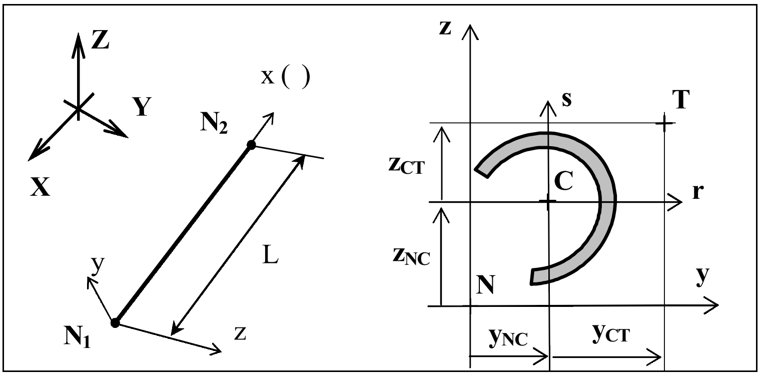

Fig. 1.

The linear kinematics of an initially straight, prismatic beam element can be described on the assumption that the cross-section undergoes a rigid body like motion in the plane normal to the centroidal axis. Accordingly, the in plane displacements of a point can be expressed by three parameters, the angle of twist θ_x^T about the longitudinal axis passing trough the **T** shear centre and the two u_y^T and u_z^T displacement components of point **T**. The axial displacement is the sum of the u_x^C axial displacement of the **C** centroid, the θ_y^C, θ_z^C rotations of planar section about the axes r and s, and the out of plane torsion warping displacement. Accordingly, the displacement vector is

$$\mathbf{u}(x, r, s, t) = [u_k] = \begin{bmatrix} u_x \\ u_y \\ u_z \end{bmatrix} = \begin{bmatrix} u_x^C + \Theta_y^C s - \Theta_z^C r - \vartheta \omega^T \\ u_y^T - \Theta_x^T (s - z_{CT}) \\ u_z^T + \Theta_x^T (r - y_{CT}) \end{bmatrix}, \tag{1}$$

where $\vartheta(x, t)$ is the warping parameter and $\omega^T(r, s)$ is the warping function, or – for thin walled sections – the sector area co-ordinate.

The geometric properties of the cross-section are

$$
\begin{aligned}
I_r &= \int_A s^2\,\mathrm{d}A, \qquad I_s = \int_A r^2\,\mathrm{d}A, \qquad I_\omega = \int_A \omega^{T^2}\,\mathrm{d}A,\\
y_{CT} &= -\frac{1}{I_r}\int_A s\omega^T\,\mathrm{d}A, \quad z_{CT} = \frac{1}{I_s}\int_A r\omega^T\,\mathrm{d}A,\\
J &= I_r + I_s + \int_A \left(s\frac{\partial\omega^T}{\partial r} - r\frac{\partial\omega^T}{\partial s}\right)\mathrm{d}A,\\
I_P &= \int_A \left[(r-y_{CT})^2 + (s-z_{CT})^2\right]\mathrm{d}A = I_s + I_r + A\left(y_{CT}^2 + z_{CT}^2\right)
\end{aligned}
\tag{2}
$$

and the principal r, s co-ordinates in *Fig. 1* were chosen so that the following integrals are zero:

$$
\begin{aligned}
&\int_A r\,\mathrm{d}A = 0, \qquad \int_A s\,\mathrm{d}A = 0, \qquad \int_A rs\,\mathrm{d}A = 0,\\
&\int_A \omega^T\,\mathrm{d}A = 0, \quad \int_A r\omega^T\,\mathrm{d}A = 0, \quad \int_A s\omega^T\,\mathrm{d}A = 0.
\end{aligned}
$$

By using the displacement (1) and the VLASZOV and BERNOULLI [7] constraints as

$$
\Theta_y^C(x,t) = -\frac{\mathrm{d}u_z^T}{\mathrm{d}x} = -u_z'^T, \quad \Theta_z^C(x,t) = \frac{\mathrm{d}u_y^T}{\mathrm{d}x} = u_y'^T, \quad \vartheta(x,t) = \frac{\mathrm{d}\Theta_x^T}{\mathrm{d}x} = \Theta_x'^T,
\tag{3}
$$

the U strain and K kinetic energy stored in a linear elastic beam element of length L are:

$$
\begin{aligned}
U &= \frac{1}{2}\int_0^L \left[EAu_x'^{C^2} + EI_r u_z''^{T^2} + EI_s u_y'^{T^2} + GJ\Theta_x'^{T^2} + EI_\omega \Theta_x''^{T^2}\right]\mathrm{d}x,\\
K &= \frac{1}{2}\int_L \Bigg[\dot u_x^{C^2} + \dot u_y^{T^2} + \dot u_z^{T^2} + \frac{I_r}{A}\dot u_z'^{T^2} + \frac{I_s}{A}\dot u_y'^{T^2} + \frac{I_\omega}{A}\dot\Theta_x'^{T^2} + \frac{I_P}{A}\dot\Theta_x^{T^2}\\
&\quad +2\left(z_{CT}\dot u_y^T\dot\Theta_x^T - y_{CT}\dot u_z^T\dot\Theta_x^T\right)\Bigg]\rho A\,\mathrm{d}x,
\end{aligned}
\tag{4}
$$

where E, G are the properties of isotropic elastic material and ρ is the mass density. The assumptions (3) imply that the shear deformations are neglected. A more detailed description of deformation including the shear effect can be found in [6] or [9].

3. Element Matrices

The derivation of element matrices is based on the assumed displacement field. A linear interpolation is adopted for the axial displacement and a cubic for the lateral deflections and the twist:

$$
\begin{aligned}
u_x^C &= u_{x1}^C(1-\xi) + u_{x2}^C\xi, \\
u_y^T(\xi) &= u_{y1}^T N_1(\xi) + \Theta_{z1}^C L N_2(\xi) + u_{y2}^T N_3(\xi) + \Theta_{z2}^C L N_4(\xi), \\
u_z^T(\xi) &= u_{z1}^T N_1(\xi) - \Theta_{y1}^C L N_2(\xi) + u_{z2}^T N_3(\xi) - \Theta_{y2}^C L N_4(\xi), \\
\Theta_x^T(\xi) &= \Theta_{x1}^T N_1(\xi) + \vartheta_1 L N_2(\xi) + \Theta_{x2}^T N_3(\xi) + \vartheta_2 L N_4(\xi),
\end{aligned}
\tag{5}
$$

in which:

$$
N_1 = 1 - 3\xi^2 + 2\xi^3, \quad N_2 = \xi - 2\xi^2 + \xi^3, \quad N_3 = 3\xi^2 - 2\xi^3,
$$
$$
N_4 = \xi^3 - \xi^2, \quad \xi = \frac{x}{L}.
$$

Define the order of the element $2 \times 7 = 14$ local displacements at the two ends as

$$
\begin{aligned}
&\underset{(14,1)}{\mathbf{U}^C}(t) \\
&= \left[u_{x1}^C,\ u_{y1}^T,\ u_{z1}^T,\ \Theta_{x1}^T,\ \Theta_{y1}^C,\ \Theta_{z1}^C,\ \vartheta_1,\ u_{x2}^C,\ u_{y2}^T,\ u_{z2}^T,\ \Theta_{x2}^T,\ \Theta_{y2}^C,\ \Theta_{z2}^C,\ \vartheta_2\right]^T.
\end{aligned}
\tag{6}
$$

Substituting interpolation (5) into (4) the expression for the potential and kinetic energy may be defined in terms of (6) local variables as

$$
U = \frac{1}{2}\mathbf{U}^{C^T}\mathbf{k}^C\mathbf{U}^C, \qquad K = \frac{1}{2}\dot{\mathbf{U}}^{C^T}\mathbf{m}^C\dot{\mathbf{U}}^C.
$$

The explicit – exactly integrated – stiffness and consistent mass matrices, $\mathbf{k}^C$ and $\mathbf{m}^C$ are given in *Appendices* **A** and **B**, respectively. The stiffness matrix – apart from sign conventions – is identical to the matrix published in [10], page 89.

The lumped mass matrix can be derived from the kinetic energy expression for an element which undergoes a rigid body like motion and rotation. The element lumped mass matrix is given in *Appendix* **C**. Here the lumped mass, due to the shear centre location, is not a diagonal matrix. Nevertheless, it is computationally much more economical than the corresponding consistent mass detailed in *Appendix* **B**.

4. Transformation from Local to Nodal Variables

The transformation which relates the (6) local variables to nodal displacements are:

$$\begin{bmatrix} u_x^C \\ u_y^T \\ u_z^T \\ \hline \Theta_x^T \\ \Theta_y^C \\ \Theta_z^C \\ \hline \vartheta \end{bmatrix} = \left[\begin{array}{ccc|ccc|c} 1 & 0 & 0 & 0 & z_{NC} & -y_{NC} & 0 \\ 0 & 1 & 0 & -(z_{NC}+z_{CT}) & 0 & 0 & 0 \\ 0 & 0 & 0 & (y_{NC}+y_{CT}) & 0 & 0 & 0 \\ \hline 0 & 0 & 0 & 1 & 0 & 0 & 0 \\ 0 & 0 & 0 & 0 & 1 & 0 & 0 \\ 0 & 0 & 0 & 0 & 0 & 0 & 0 \\ \hline 0 & 0 & 0 & 0 & 0 & 0 & 1 \end{array}\right] \begin{bmatrix} u_x^N \\ u_y^N \\ u_z^N \\ \hline \Theta_x^N \\ \Theta_y^N \\ \Theta_z^N \\ \hline \vartheta \end{bmatrix} \tag{7}$$

Using the above transformation at each node the stiffness and mass matrix can be transformed to the local x, y, z system in the corresponding mesh node. Finally, the element stiffness and mass matrices evaluated in the local x, y, z system are transformed to the global X, Y, Z structural system in a usual manner. A detailed description of the (7) transformation process can be found in [8].

5. Numerical Examples

In order to examine the validity and accuracy of the lumped mass formulation, the vibration analysis of a simply supported and a cantilever beam is conducted. Numerical solutions of the present study are compared with the analytical and COSMOS/M shell element results.

5.1. *Simply Supported Beam*

Material and sectional properties used in this example are listed in *Fig.2*. Closed form solution for the torsional vibration with free end warping is known as [1]:

$$\alpha_n = \frac{n}{2L}\sqrt{\frac{GJ}{\rho\,(I_r+I_s)}}\sqrt{\frac{1+n^2\dfrac{\pi^2 EI_\omega}{L^2GJ}}{1+n^2\dfrac{\pi^2 I_\omega}{L^2\,(I_r+I_s)}}}, \qquad n = 1, 2, \ldots. \tag{8}$$

The beam was analysed with different m number of elements. At the end nodes $(x = 0, L)$ in addition to the normal hinged support conditions the 7th warping parameter was left free. *Tables 1a* and *1b* show that the torsional frequencies – even for a coarse mesh and lumped mass – are in good agreement with the (8) analytical solution. As the convergence study shows that $m = 20$ element number is sufficient to get a reasonable accuracy and number of modes, this mesh is used in the subsequent problems.

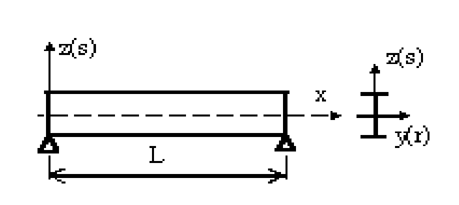

$L = 2000$ mm
$A = 2848$ mm^2
$I_r = 1.943\ e^7$ mm^4
$I_s = 1.423\ e^6$ mm^4
$J = 6.847\ e^4$ mm^4
$I_\omega = 1.274\ e^{10}$ mm^4

$E = 2.0\ e^5$ N/mm^2
$G = 0.8\ e^5$ N/mm^2
$\nu = 0.25$
$\rho = 8.0$ N sec^2/mm^4

Fig. 2. Simply supported beam with doubly symmetric section

Table 1a. Convergence of torsional frequencies (Hz), with *consistent* mass matrix. 7 DOF results with free end warping

n	$m = 2$	$m = 4$	$m = 8$	$m = 16$	$m = 20$	analitical
1	66.485	66.349	66.340	66.339	66.339	66.339
2		214.29	213.63	213.59	213.59	213.59
3		462.00	454.91	454.41	454.39	454.37
4			790.89	788.13	788.01	787.93
5			1222.5	1212.4	1212.0	1211.6

Table 1b. Convergence of torsional frequencies (Hz), with *lumped* mass matrix. 7 DOF results with free end warping.

n	$m = 2$	$m = 4$	$m = 8$	$m = 16$	$m = 20$	analitical
1	65.601	66.309	66.338	66.339	66.339	66.339
2		211.83	213.51	213.58	213.59	213.59
3		425.59	453.54	454.33	454.36	454.37
			782.73	787.71	787.84	787.93
5			1187.8	1210.8	1211.3	1211.6

5.2. *Cantilever*

To illustrate the importance of internal and external warping constraint and the performance of the lumped mass matrix, the results of two test problems with the same material properties are detailed herein: a straight cantilever with (1) a double symmetric I and (2) with U section. In each case the beam structure was analysed with a 20-element mesh. A comparison was made with the classic – neglected warping effect – beam frequency solutions (columns A in *Tables* 2, 3a):

bending:

$$\alpha_n = \frac{\Gamma_n}{2\pi L^2}\sqrt{\frac{IE}{A\rho}}, \quad \Gamma_1 = 1.875^2, \quad \Gamma_2 = 4.694^2, \quad \Gamma_2 = 7.855^2, \tag{9a}$$

torsion:

$$\alpha_n = \frac{2n-1}{4L}\sqrt{\frac{GJ}{\rho\,(I_r + I_s)}}, \quad n = 1, 2, \ldots \tag{9b}$$

and the results of 6 DOF beam element model (columns B in *Tables* 2, 3a). Moreover, the frequencies of the beam like modes obtained by COSMOS/M thick shell finite element model are listed in 'SHELL' columns in *Tables* 2 and 3b. The cantilevers were modelled by using 1280 (U section) and 1600 (I section) four-noded thick shell elements.

(1) I section

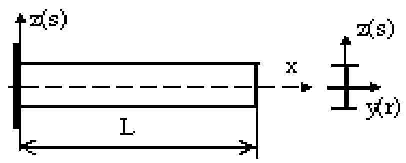

IPE 200
$L = 2000$ mm
$A = 2848$ mm^2
$I_r = 1.943\,e^7$ mm^4
$I_s = 1.423\,e^6$ mm^4
$J = 6.847\,e^4$ mm^4
$I_\omega = 1.274\,e^{10}$ mm^4

$E = 2.0\,e^5$ N/mm^2
$G = 0.8\,e^5$ N/mm^2
$\nu = 0.25$
$\rho = 8.0$ N sec^2/mm^4

Fig. 3. Cantilever with doubly symmetric section

Table 2. Test problem 1, torsional frequencies (Hz), 6 DOF results (B) and 7 DOF results with free end warping (C) and constrained end warping (D).

	A	B(cons)	B(lump)	C(cons)	C(lump)	D(cons)	D(lump)	SHELL
1	22.650	22.650	22.650	23.889	23.881	33.516	33.494	30.29
2	67.951	67.951	67.938	105.91	105.62	135.03	134.55	127.4
3	113.25	113.25	113.17	272.59	271.05	326.85	324.78	317.3
4	158.55	158.55	158.26	533.82	532.74	612.39	606.89	
5	203.85	203.85	203.05	887.57	878.31	989.69	978.28	
6	249.15	249.16	247.31	1330.6	1312.7	1455.5	1435.0	

The comparison of results in columns A, B with others in C, D shows the significant effect of warping inertia and internal (C) and external (D) warping constraints on torsional vibration.

(2) U section

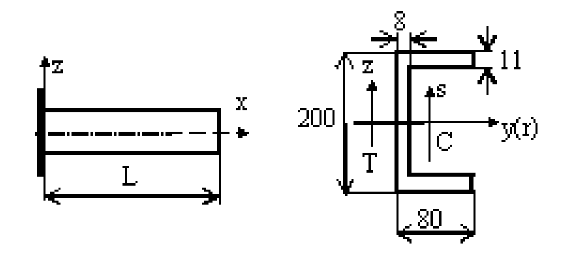

U 200
$L = 2000$ mm
$A = 3157$ mm^2
$I_r = 1.972\, e^7$ mm^4
$I_s = 1.955\, e^6$ mm^4
$J = 1.025\, e^4$ mm^4
$I_\omega = 1.227\, e^{10}$ mm^4
$y_{CT} = -48.7$ mm

Fig. 4. Cantilever with a channel section

Table 3a. Test problem 2, frequencies (Hz), 6 DOF results (B). by$i$, bz$i$ bending, ti torsion, ai longitudinal modes.

n	mode	A	B (cons)	B (lump)
1	by1	17.379	17.375	17.355
2	t1	26.635	26.635	26.635
3	bz1	54.720	54.533	54.471
4	t2	79.906	79.906	79.891
5	by2	108.92	108.66	108.23
6	t3	133.18	133.18	133.08
7	t4	186.45	186.45	186.11
8	t5	239.72	239.72	238.78
9	t6	292.99	292.99	290.82
10	by3	305.02	303.02	301.25
19	a1	625.00	625.16	624.84

The modes – except the by$i$ bending modes – in consequence of the eccentric position of the shear centre exhibit strong flexural bending coupling. This coupling phenomenon cannot be predicted by the classic 6 DOF finite element model.

All the numerical results prove the good accuracy of the simple lumped mass matrix.

Table 3b. Test problem 2, frequencies (Hz), 7 DOF results with free end warping (C) and constrained end warping (D). by$i$, bz$i$ bending, ti torsion, ai longitudinal modes.

	mode	C(cons)	C(lump)	mode	D(cons)	D(lump)	mode	SHELL
1	by1	17.375	17.355	by1	17.375	17.355	by1	17.31
2	bz+t1	23.314	23.306	bz+t1	30.198	30.182	bz+t1	29.57
3	bz+t2	63.876	63.791	bz+t2	66.630	66.535	bz+t2	65.34
4	bz+t3	98.621	98.324	by2	108.66	108.23	by2	105.83
5	by2	108.66	108.23	bz+t3	119.90	119.45	bz+t3	116.14
6	bz+t4	234.78	233.44	bz+t4	279.27	277.40	bz+t4	269.83
7	by3	303.20	301.25	by3	303.20	301.25		
8	bz+t5	391.58	390.43	bz+t5	392.24	391.44		
9	bz+t6	453.22	494.43	bz+t6	517.44	512.14		
10	by4	591.23	585.93	by4	591.23	585.93		
11	a1	625.16	624.84	a1	625.16	624.84		

Acknowledgements:

The present research was supported by Széchenyi-NKFP (Hungarian National Research and Development Found) Grant no: 2002/16.

References

[1] VLASOV, V. Z., Thin Walled Elastic Beams, 2$^{\text{nd}}$ ed. Israel Program for Scientific Transactions, Jerusalem, 1961.
[2] TIMOSHENKO, S. P. – GERE, J. M., *Theory of Elastic Stability*, 2$^{\text{nd}}$ ed. McGraw Hill, New-York, 1961.
[3] FRIBERG, P. O., Coupled Vibration of Beams – an Exact Dynamic Element Stiffness Matrix, *Int. J. Numerical Methods in Engng*, **19** (1993), pp. 479–493.
[4] BANERJEE, J. R. – GUO, S. – HOWSON, W. P., Exact Dynamic Stiffness Matrix of a Bending-Torsion Coupled Beam Including Warping, *Computers and Structures*, **59** (1996), pp. 613–621.
[5] TRAHAIR, N. S. – PI, Y-L., Torsion, Bending and Buckling of Steel Beams, *Engineering Structures*, **19** (1997), pp. 372–377.
[6] KIM, S. B. – KIM, M. Y., Improved Formulation for Spatial Stability and Free Vibration of Thin-Walled Tapered Beams and Space Frames, *Engineering Structures*, **22** (2000), pp. 446–458.
[7] WEMPNER, G., *Mechanics of Solids with Application to Thin Bodies*, Sijthoff Noordhoff, 1981.
[8] KISS, F., A New Aspects for the Use of Thin-Walled Beams as Shell Stiffeners as Spacecraft Structures, *Proc. of Conf. on Spacecraft Structures and Mechanical Testing*, Noordwijk, The Netherlands, October 19–21, 1987, pp. 455–459.
[9] VÖRÖS, G. M., A Special Purpose Element for Shell-Beam Systems, *Computers and Structures*, **29** (1988), pp. 301–308.

[10] KITIPORNCHAI, S. – CHAN, S. L., Stability and Non-Linear Finite Element Analysis of Thin-Walled Structures, in *Finite Element Applications to Thin-Walled Structures*, ed. Bull, J.W. Elsevier. 1989.

[11] KOUHIA, R. – TUOMALA, M., Static and Dynamic Analysis of Space Frames Using Simple Timoshenko Type Elements, *Int. J. Numerical Methods in Engng.*, **36** (1993), pp. 1189–1221.

Appendix A

The 14×14 linear stiffness matrix $\mathbf{k}^C$ is symmetric. Only the upper triangle is given here.

$$
\mathbf{k}^C = \left[\begin{array}{ccccccc|ccccccc}
a & 0 & 0 & 0 & 0 & 0 & 0 & -a & 0 & 0 & 0 & 0 & 0 & 0 \\
 & b & 0 & 0 & 0 & c & 0 & 0 & -b & 0 & 0 & 0 & c & 0 \\
 & & d & 0 & -e & 0 & 0 & 0 & 0 & -d & 0 & -e & 0 & 0 \\
 & & & f & 0 & 0 & g & 0 & 0 & 0 & -f & 0 & 0 & g \\
 & & & & 2h & 0 & 0 & 0 & 0 & e & 0 & h & 0 & 0 \\
 & & & & & 2i & 0 & 0 & -c & 0 & 0 & 0 & i & 0 \\
 & & & & & & j & 0 & 0 & 0 & -g & 0 & 0 & k \\
\hline
 & & & & & & & a & 0 & 0 & 0 & 0 & 0 & 0 \\
 & & & & & & & & b & 0 & 0 & 0 & -c & 0 \\
 & & & & & & & & & d & 0 & e & 0 & 0 \\
 & & & & & & & & & & f & 0 & 0 & -g \\
 & & & & & & & & & & & 2h & 0 & 0 \\
 & & & & & & & & & & & & 2i & 0 \\
 & & & & & & & & & & & & & j
\end{array}\right]
$$

$$
a = \frac{EA}{L}, \quad b = \frac{12EI_s}{L^3}, \quad c = \frac{6EI_s}{L^2}, \quad d = \frac{12EI_r}{L^3},
$$
$$
e = \frac{6EI_r}{L^2}, \quad f = \frac{6GJ}{5L} + \frac{12EI_\omega}{L^3}, \quad g = \frac{GJ}{10} + \frac{6EI_\omega}{L^2}, \quad h = \frac{2EI_r}{L},
$$
$$
i = \frac{2EI_s}{L}, \quad j = \frac{2GJL}{15} + \frac{4EI_\omega}{L}, \quad k = -\frac{GJL}{30} + \frac{2EI_\omega}{L}.
$$

Appendix B

The 14×14 *consistent* mass matrix. $\underset{(14,14)}{\mathbf{m}^C} = \rho AL \begin{bmatrix} \mathbf{m}_1 & \mathbf{m}_{12} \\ \mathbf{m}_{12}^T & \mathbf{m}_2 \end{bmatrix}$,

$$
\underset{(7,7)}{\mathbf{m}_1} = \left[\begin{array}{ccc|ccc|c}
2a & 0 & 0 & 0 & 0 & 0 & 0 \\
 & b + ki_s^2 & 0 & bz_{CT} & 0 & f + mi_s^2 & fz_{CT} \\
 & & b + ki_r^2 & -by_{CT} & -f - mi_r^2 & 0 & fy_{CT} \\
\hline
 & & & bi_p^2 + ki_\omega^4 & -fy_{CT} & fz_{CT} & fi_p^2 + mi_\omega^4 \\
 & & & & h + 4ei_r^2 & 0 & hy_{CT} \\
 & & & & & h + 4ei_s^2 & hz_{CT} \\
\hline
 & & & & & & hi_p^2 + 4ei_\omega^4
\end{array}\right]
$$

$$
\underset{(7,7)}{\mathbf{m}_2} = \left[\begin{array}{ccc|ccc|c}
2a & 0 & 0 & 0 & 0 & 0 & 0 \\
 & b + ki_s^2 & 0 & bz_{CT} & 0 & -f - mi_s^2 & -fz_{CT} \\
 & & b + ki_r^2 & -by_{CT} & f + mi_r^2 & 0 & -fy_{CT} \\
\hline
 & & & bi_p^2 + ki_\omega^4 & fy_{CT} & -fz_{CT} & -fi_p^2 - mi_\omega^4 \\
 & & & & h + 4ei_r^2 & 0 & hy_{CT} \\
 & & & & & h + 4ei_s^2 & hz_{CT} \\
\hline
 & & & & & & hi_p^2 + 4ei_\omega^4
\end{array}\right]
$$

$$
\underset{(7,7)}{\mathbf{m}_{12}} = \left[\begin{array}{ccc|ccc|c}
a & 0 & 0 & 0 & 0 & 0 & 0 \\
0 & c - ki_s^2 & 0 & cz_{CT} & 0 & -g + mi_s^2 & -gz_{CT} \\
0 & 0 & c - ki_r^2 & -cy_{CT} & g - ji_r^2 & 0 & -gy_{CT} \\
\hline
0 & cz_{CT} & -cy_{CT} & ci_p^2 - ki_\omega^4 & gy_{CT} & -gz_{CT} & -gi_p^2 + mi_\omega^4 \\
0 & 0 & -g + mi_r^2 & -gy_{CT} & -j - ei_r^2 & 0 & -jy_{CT} \\
0 & g - mi_s^2 & 0 & gz_{CT} & 0 & -j - ei_s^2 & -jz_{CT} \\
\hline
0 & gz_{CT} & gy_{CT} & gi_p^2 - mi_\omega^4 & -jy_{CT} & -jz_{CT} & -ji_p^2 - ei_\omega^4
\end{array}\right]
$$

$$
a = \frac{1}{6}, \quad b = \frac{13}{35}, \quad c = \frac{9}{70}, \quad e = \frac{1}{30}, \quad f = \frac{11L}{210}
$$

$$
g = \frac{13L}{420}, \quad h = \frac{L^2}{105}, \quad j = \frac{L^2}{140}, \quad k = \frac{6}{5L^2}, \quad m = \frac{1}{10L}.
$$

$$
i_r^2 = \frac{I_r}{A}, \quad i_s^2 = \frac{I_s}{A}, \quad i_p^2 = i_r^2 + i_s^2 + y_{CT}^2 + z_{CT}^2, \quad i_\omega^4 = \frac{I_\omega}{A}.
$$

Appendix C

The 14×14 *lumped* mass matrix.

$$\underset{(14,14)}{\mathbf{m}^C} = \begin{bmatrix} \mathbf{m} & \mathbf{0} \\ \mathbf{0} & \mathbf{m} \end{bmatrix}, \qquad \underset{(7,7)}{\mathbf{m}} = \frac{\rho AL}{2} \left[\begin{array}{ccc|cccc|c} 1 & 0 & 0 & 0 & 0 & 0 & 0 \\ & 1 & 0 & z_{CT} & 0 & 0 & 0 \\ & & 1 & -y_{CT} & 0 & 0 & 0 \\ \hline & & & i_P^2 & 0 & 0 & 0 \\ & & & & i_r^2 & 0 & 0 \\ & & & & & i_s^2 & 0 \\ \hline & & & & & & i_\omega^4 \end{array} \right]$$